Cell Reports, Volume *43*

Supplemental information

GCN2 is a determinant of the response to WEE1 kinase inhibition in small-cell lung cancer

Alexandros P. Drainas, Wen-Hao Hsu, Alec E. Dallas, Carson D. Poltorack, Jun W. Kim, Andy He, Garry L. Coles, Maya Baron, Michael C. Bassik, and Julien Sage

Figure S1

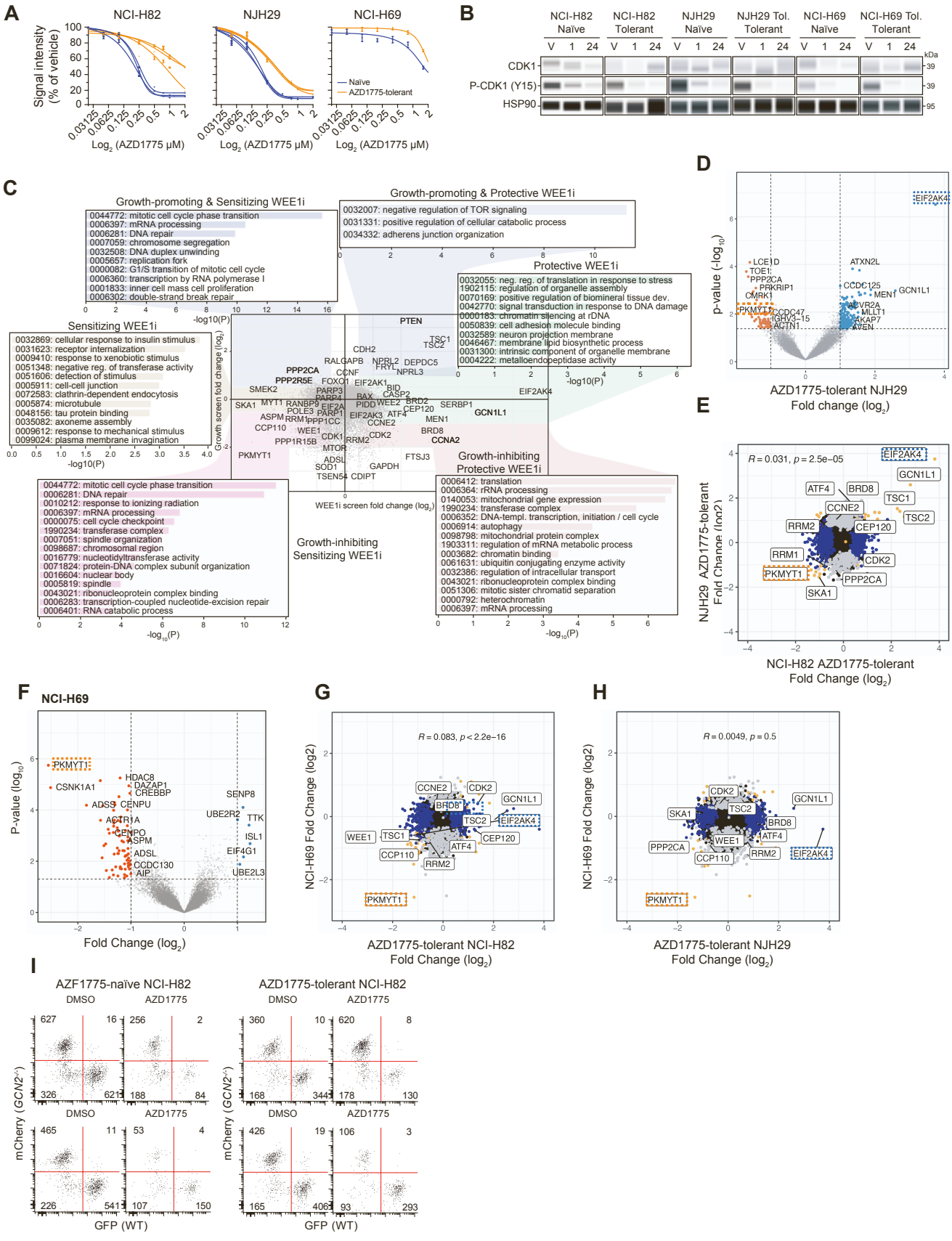
A
NCI-H82
NJH29
NCI-H69
Signal intensity (% of vehicle)
Naïve
AZD1775-tolerant
Log2 (AZD1775 μM)
B
NCI-H82 Naïve
NCI-H82 Tolerant
NJH29 Naïve
NJH29 Tol. Tolerant
NCI-H69 Naïve
NCI-H69 Tol. Tolerant
V 1 24
kDa
CDK1
P-CDK1 (Y15)
HSP90
C
Growth-promoting & Sensitizing WEE1i
0044772: mitotic cell cycle phase transition
0006397: mRNA processing
0006281: DNA repair
0007059: chromosome segregation
0032508: DNA duplex unwinding
0005657: replication fork
0000082: G1/S transition of mitotic cell cycle
0006360: transcription by RNA polymerase I
0001833: inner cell mass cell proliferation
0006302: double-strand break repair
-log10(P)
Growth-promoting & Protective WEE1i
0032007: negative regulation of TOR signaling
0031331: positive regulation of cellular catabolic process
0034332: adherens junction organization
Protective WEE1i
0032055: neg. reg. of translation in response to stress
1902115: regulation of organelle assembly
0070169: positive regulation of biomineral tissue dev.
0042770: signal transduction in response to DNA damage
0000183: chromatin silencing at rDNA
0050839: cell adhesion molecule binding
0032589: neuron projection membrane
0046467: membrane lipid biosynthetic process
0031300: intrinsic component of organelle membrane
0004222: metalloendopeptidase activity
Sensitizing WEE1i
0032869: cellular response to insulin stimulus
0031623: receptor internalization
0009410: response to xenobiotic stimulus
0051348: negative reg. of transferase activity
0051606: detection of stimulus
0005911: cell-cell junction
0072583: clathrin-dependent endocytosis
0005874: microtubule
0048156: tau protein binding
0035082: axoneme assembly
0009612: response to mechanical stimulus
0099024: plasma membrane invagination
Growth screen fold change (log2)
PTEN
TSC1
TSC2
CDH2
RALGAPB
NPRL2
DEPDC5
FRYL
PPP2CA
CCNF
NPRL3
PPP2R5E
FOXO1
EIF2AK1
SMEK2
PARP3
BID
PARP4
BAX
CASP2
EIF2AK4
SKA1
MYT1
RANBP9
PIDD
WEE2
BRD2
POLE3
EIF2A
PARP1
CEP120
SERBP1
ASPM
RRM1
PPP1CC
EIF2AK3
ATF4
CCNE2
MEN1
GCN1L1
CCP110
WEE1
BRD8
CDK1
RRM2
CDK2
CCNA2
PPP1R15B
MTOR
PKMYT1
ADSL
FTSJ3
SOD1
GAPDH
TSEN54
CDIPT
WEE1i screen fold change (log2)
Growth-inhibiting Protective WEE1i
0006412: translation
0006364: rRNA processing
0140053: mitochondrial gene expression
1990234: transferase complex
0006352: DNA-templ. transcription, initiation / cell cycle
0006914: autophagy
0098798: mitochondrial protein complex
1903311: regulation of mRNA metabolic process
0003682: chromatin binding
0061631: ubiquitin conjugating enzyme activity
0032386: regulation of intracellular transport
0043021: ribonucleoprotein complex binding
0051306: mitotic sister chromatid separation
0000792: heterochromatin
0006397: mRNA processing
Growth-inhibiting Sensitizing WEE1i
0044772: mitotic cell cycle phase transition
0006281: DNA repair
0010212: response to ionizing radiation
0006397: mRNA processing
0000075: cell cycle checkpoint
1990234: transferase complex
0007051: spindle organization
0098687: chromosomal region
0016779: nucleotidyltransferase activity
0071824: protein-DNA complex subunit organization
0016604: nuclear body
0005819: spindle
0043021: ribonucleoprotein complex binding
0006283: transcription-coupled nucleotide-excision repair
0006401: RNA catabolic process
D
p-value (-log10)
EIF2AK4
LCE1D
TOE1
PPP2CA
PPKRIP1
CMRK1
PKMYT1
CCDC47
IGHV3-15
ACTN1
ATXN2L
CCDC125
MEN1
GCN1L1
ADCY2R2A
MLLT1
AKAP7
AVEN
AZD1775-tolerant NJH29
Fold change (log2)
E
R = 0.031, p = 2.5e−05
EIF2AK4
GCN1L1
ATF4
BRD8
TSC1
CCNE2
TSC2
RRM2
CEP120
RRM1
CDK2
PKMYT1
PPP2CA
SKA1
NJH29 AZD1775-tolerant Fold Change (log2)
NCI-H82 AZD1775-tolerant Fold Change (log2)
F
NCI-H69
P-value (log10)
PKMYT1
CSNK1A1
HDAC8
DAZAP1
CREBBP
ADSS
CENPU
ACTR1A
CENPO
ASPM
ADSL
CCDC130
AIP
SENP8
UBE2R2
TTK
ISL1
EIF4G1
UBE2L3
Fold Change (log2)
G
R = 0.083, p < 2.2e−16
CCNE2
CDK2
BRD8
GCN1L1
TSC2
EIF2AK4
WEE1
TSC1
CEP120
ATF4
CCP110
RRM2
PKMYT1
NCI-H69 Fold Change (log2)
AZD1775-tolerant NCI-H82 Fold Change (log2)
H
R = 0.0049, p = 0.5
CDK2
GCN1L1
SKA1
TSC2
BRD8
ATF4
WEE1
PPP2CA
RRM2
CCP110
EIF2AK4
PKMYT1
NCI-H69 Fold Change (log2)
AZD1775-tolerant NJH29 Fold Change (log2)
I
AZF1775-naïve NCI-H82
AZD1775-tolerant NCI-H82
DMSO
AZD1775
627 16 326 621
256 2 188 84
360 10 168 344
620 8 178 130
465 11 226 541
53 4 107 150
426 19 165 406
106 3 93 293
mCherry (GCN2-/-)
GFP (WT)

Figure S1, related to Figure 1. Characterization of the response of human SCLC cell lines to AZD1775 treatment and overview of the genome-wide CRISPR/Cas9 screens.

(A) AlamarBlue cell viability assays with naïve SCLC cell lines and the same cell lines selected to be more tolerant to AZD1775 by growth in increasing concentrations of this drug in response to different concentrations of AZD1775 (2 μM to 0.03125 μM for 5 days). N=3 for NCI-H82 and NJH29 naïve and AZD1775-tolerant cells (6 replicates per condition); n=1 for NCI-H69 naïve and AZD1775-tolerant cells (6 replicates per condition).

(B) Immunoassay for CDK1 and CDK1 phosphorylated at tyrosine 15 (Y15) in response to AZD1775 treatment (1 hr or 24 hr, NCI-H82 and NJH29: 0.4 μM; rest 0.8 μM), compared to vehicle-treated cells (V, 1 hr) in naïve and AZD1775-tolerant SCLC cell lines (n=1). HSP90 is a loading control. Y15 is the direct target of WEE1 on CDK1.

(C) Gene ontology of six categories (as noted) from the fold change between the AZD1775 vs. DMSO comparison (day 21) and the day 0 vs. day 21 comparison (DMSO condition) in the CRISPR/Cas9 screens for NCI-H82 tolerant cells. As an example, “Protective WEE1i” means protective effects of the gene knockout in the screen when cells are treated with AZD1775.

(D) Enrichment of genes from AZD1775-tolerant NJH29 cells in a genome-wide CRISPR/Cas9 screen (AZD1775 vs. Control, day 21), as in Figure 1B with NCI-H82 cells.

(E) Correlation of the fold change values from the CRISPR/Cas9 screens in AZD1775-tolerant NJH29 and AZD1775-tolerant NCI-H82 cells.

(F) Enrichment of genes from AZD1775-tolerant NCI-H69 cells in a genome-wide CRISPR/Cas9 screen (AZD1775 vs. Control, day 21), as in Figure 1B with NCI-H82 cells.

(G) Correlation of the fold change values from the CRISPR/Cas9 screens in AZD1775-tolerant NCI-H69 and AZD1775-tolerant NCI-H82 cells.

(H) Correlation of the fold change values from the CRISPR/Cas9 screens in AZD1775-tolerant NCI-H69 and AZD1775-tolerant NJH29 cells.

(I) Representative flow cytometry analysis in competition assays between naïve and tolerant NCI-H82 cells: *GCN2*$^{-/-}$ or *CReP*$^{-/-}$ cells were labeled with a lentiviral vector expressing mCherry while control wild-type cells were labeled with lentiviral vector expressing GFP.

Supplemental Figure 2

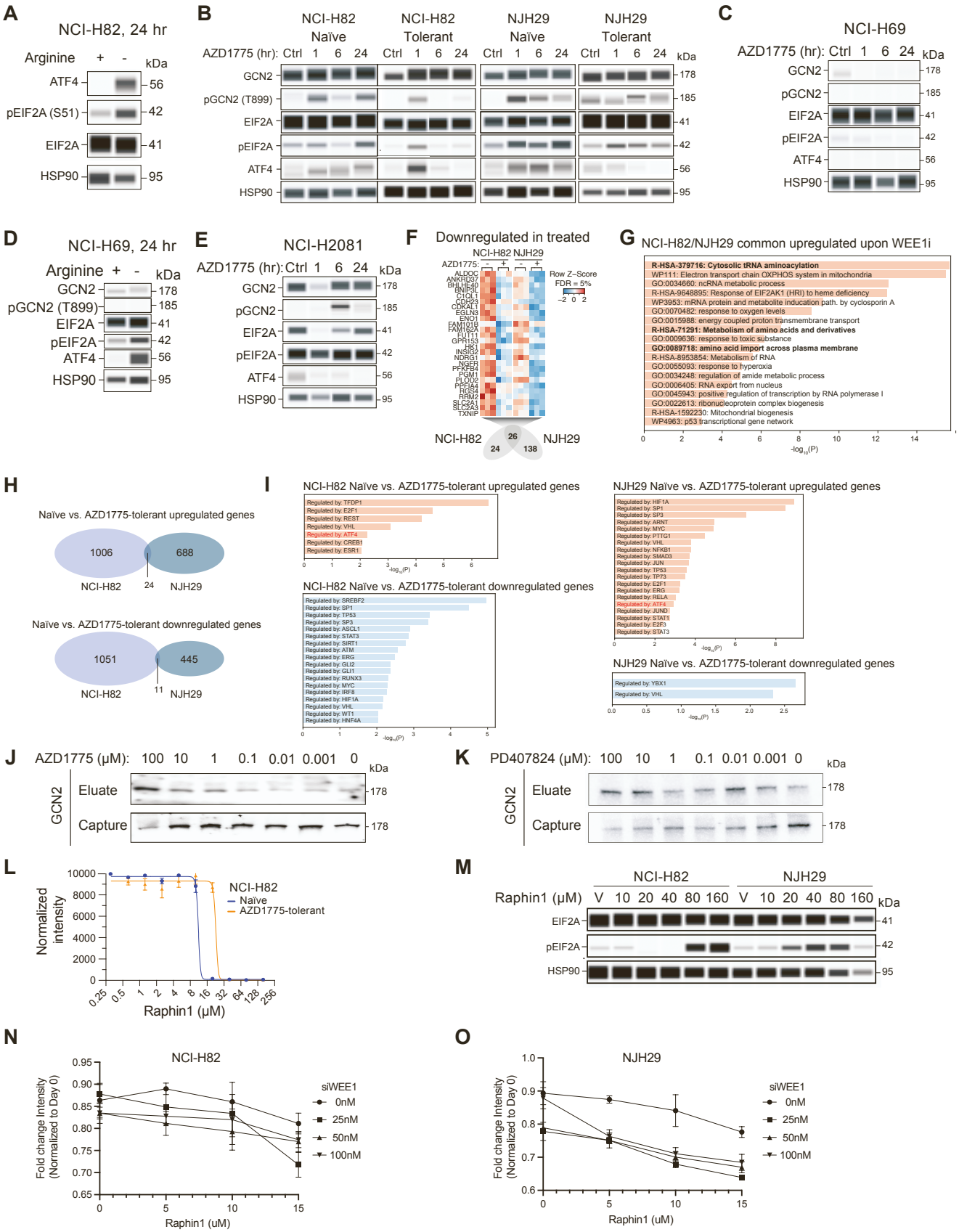

Figure S2, related to Figure 2. GCN2 activity in different SCLC cell lines upon WEE1 kinase inhibition.

(A) Analysis of the GCN2 pathway by immunoassay in NCI-H82 cells (AZD1775-naïve) in response to arginine starvation. HSP90 is a loading control (n=1).

(B) Analysis of the GCN2 pathway by immunoassay with AZD1775 treatment (0.4 μM) in NCI-H82 and NJH29 naïve and AZD1775-tolerant cells. Control: DMSO at 1 hour. HSP90 is a loading control (n=1 per cell line).

(C) As in (B) with NCI-H69 cells and 0.8 μM AZD1775.

(D) As in (A) with NCI-H69 cells.

(E) As in (B) with NCI-H2081 cells and 0.8 μM AZD1775.

(F) Commonly downregulated genes in an RNA-seq analysis of NCI-H82 and NJH29 cells (n=3 per condition) after a 24-hour treatment with AZD1775 (0.4 μM). Heatmaps indicate gene counts in each replicate.

(G) GO term analysis for commonly upregulated gene in NCI-H82 or NJH29 after a 24-hour treatment with AZD1775 (0.4 μM) (n=3 per condition).

(H) Differentially regulated genes between naïve and AZD1775-tolerant NCI-H82 and NJH29 cells following RNA-seq analysis (p-adj < 0.05).

(I) Enrichment analysis of transcription factors using TRRUST transcriptional regulatory database using differentially regulated genes between naïve and AZD1775-tolerant NCI-H82 and NJH29 cells. ATF4 is highlighted in red.

(J) Immunoblot for GCN2 on the eluate and captured fractions with different concentrations of AZD1775.

(K) Immunoblot for GCN2 on the eluate and captured fractions with different concentrations of PD407824.

(L) Raphin1 titration in naïve and AZD1775-tolerant NCI-H82 cells measured by alamarBlue assays, SEM (n=6).

(M) Analysis of the EIF2A phosphorylation by immunoassay in NCI-H82 cells and NJH29 cells (AZD1775-naïve) upon increasing concentrations of Raphin1 (0-256 μM) (n=1).

(N) Raphin1 titration in NCI-H82 cells treated with different concentrations of siRNA targeting WEE1 (siWEE1).

(O) Raphin1 titration in NJH29 cells treated with different concentrations of siWEE1 (n=3, SEM).

Supplemental Figure 3

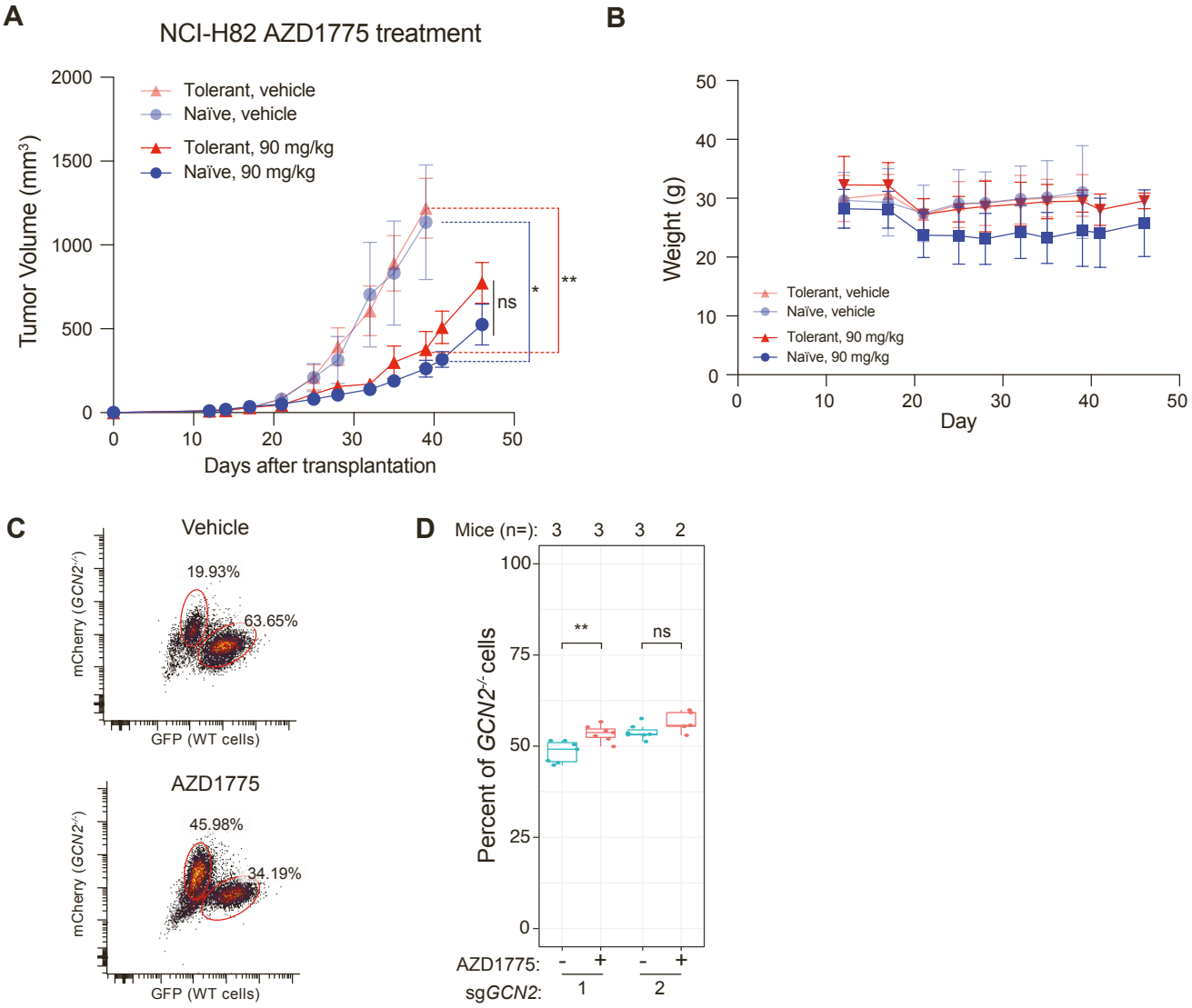

Figure S3, related to Figure 3. AZD1775 treatment reduces SCLC tumor growth.

(A) Tumor growth of NCI-H82 cells in subcutaneous tumors in NSG mice with vehicle or AZD1775 treatment (90 mg/kg, dosed by oral gavage for 5 days followed by a 2-day break per week). Mice per group: Tolerant vehicle: n=4; Naïve vehicle: n=4; Tolerant treated: n=3; Naïve treated: n=4; n=1 experiment. T-Test, p-value: 0.05-0.01 (*), 0.01-0.001 (**), < 0.001 (***).

(B) Body weight of mice as in (A).

(C) Representative flow cytometry data for the *in vivo* competition assays. Cell populations displayed and percentage of cells in each gate.

(D) *In vivo* competition assay with *GCN2*$^{-/-}$ (mCherry^{+}) and WT (GFP^{+}) NCI-H82 cells. Percent of *GCN2*$^{-/-}$ cells are displayed between the treated group and untreated group. T-Test, p-value: 0.05-0.01 (*), 0.01-0.001 (**), < 0.001 (***). Mouse numbers per condition indicated in plot.